

On JT gravity path integrals and the tunneling process

Hamed Zolfi^{a,b} and Mohsen Alishahiha^c

^a Department of Physics, College of Science, Shiraz University, Shiraz 71454, Iran

^b School of Particles and Accelerators, Institute for Research in Fundamental Sciences (IPM)
P.O. Box 19395-5531, Tehran, Iran

^c School of Quantum Physics and Matter, Institute for Research in Fundamental Sciences
(IPM), P.O. Box 19395-5531, Tehran, Iran

Emails: h.zolfi@saadi.shirazu.ac.ir, alishah@ipm.ir

Abstract

The Jackiw-Teitelboim (JT) gravity path integral of the trumpet can be interpreted as a transition amplitude from an older black hole to a younger one, accompanied by the emission of a baby universe, represented by the geodesic boundary of the trumpet. However, this interpretation becomes less straightforward for geometries with higher genus and multiple geodesic boundaries. In this paper, we examine the path integral for these more complex geometries and find that maintaining this interpretation requires accounting for a portion of the moduli space.

Contents

1	Introduction	2
2	Tunneling in a geometry with constant Weil-Petersson volume	5
2.1	Kontsevich’s decomposition of moduli space	5
2.2	Geometry with two baby universes	7
3	Tunneling in geometries with nontrivial Weil-Petersson volumes	9
3.1	Geometry with three baby universes	10
3.2	Single-genus geometry with a baby universe	13
4	Concluding remarks	15
A	Kontsevich graphs of four-holed sphere	16

1 Introduction

The role of spacetime wormholes in the study of quantum gravity has attracted considerable attention in recent years, particularly about the Mathur/AMPS firewall paradox, which raises fundamental questions about the black hole information paradox and the nature of spacetime [1–11].

Within the framework of JT gravity [12–17]¹, intriguing connections have emerged between wormholes and firewalls. These connections suggest that the formation of wormholes could lead to the generation of firewalls through the emission of large baby universes at late times [21, 22]². The emission of a baby universe from the wormhole causes a shortening of its length, which in turn leads to the formation of a firewall. Black hole firewalls exhibit characteristics similar to those of white holes [25], suggesting a compelling scenario in which an aging black hole could tunnel into a white hole or firewall by emitting large baby universes. The exploration of this phenomenon has been conducted within the context of JT gravity, initially for genus-one topologies, where the emission is associated with the production of a single baby universe [21]. Subsequent investigations have extended this analysis to higher-genus scenarios, revealing that the emission can involve an arbitrary number of baby universes [26].

¹JT gravity is not dual to an ordinary quantum system on the asymptotic boundary of spacetime, as one might expect from prior holographic duality, but rather to a matrix model, which is a random ensemble of quantum mechanical systems [18–20].

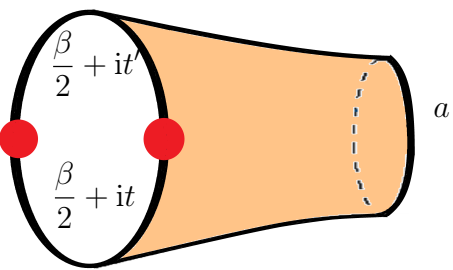
²It is worth noting that Coleman, Giddings, and Strominger established the connection between the physics of spacetime wormholes and baby universes in the 1980s [23, 24].

Since the volume of a black hole’s interior (or wormhole) is linearly proportional to its age [27–33]³, one could argue that the emission of a baby universe effectively makes the black hole younger. To explore this concept within the framework of JT gravity, one observes that through a specific analytic continuation, the trumpet partition function in JT gravity can be interpreted as a tunneling amplitude between states of different ages [21]. To be more precise, let us examine the explicit expression of the partition function for the trumpet geometry in JT gravity [19]:

$$Z_{\text{trumpet}}(\beta, a) = \frac{\exp\left(-\frac{a^2}{4\beta}\right)}{\sqrt{4\pi\beta}}, \quad (1.1)$$

where β is the renormalized length of the Euclidean AdS boundary and a is the length of the geodesic boundary (baby universe) of the trumpet. Let us now consider the analytic continuation $\beta \rightarrow \beta + i(t - t')$. This transformation allows us to interpret the trumpet path integral as a tunneling amplitude from the thermofield double state of age t to the thermofield double state of age t' , along with the creation of a baby universe of size a , as demonstrated in the following relation:

$\langle \text{age } t'; a | \text{age } t \rangle =$



$$= \frac{\exp\left(-\frac{a^2}{4(\beta + i(t - t'))}\right)}{\sqrt{4\pi(\beta + i(t - t'))}} \approx \frac{\exp\left(i\frac{a^2}{4(t - t')} - \beta\frac{a^2}{4(t - t')^2}\right)}{\sqrt{4\pi i(t - t')}}. \quad (1.2)$$

It is useful to examine this amplitude at a fixed energy, which can be achieved by employing an inverse Laplace transform. To do this, we multiply the amplitude by $e^{\beta E}$ and integrate over β along an inverse Laplace transform contour. This procedure results in a delta function, yielding:

$$2\sqrt{E}(t - t') = \pm a. \quad (1.3)$$

Discarding the minus sign due to its unphysical implications [21], we define the wormhole lengths before and after emitting a baby universe as $\ell = 2\sqrt{E}t$ and $\ell' = 2\sqrt{E}t'$, respectively. Then the above equation can be expressed as:

$$\ell = \ell' + a, \quad (1.4)$$

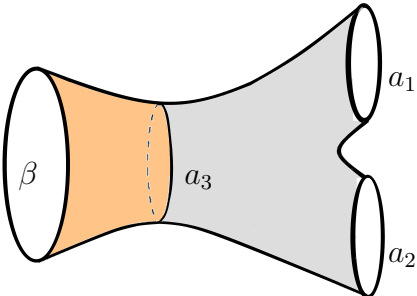
which can be interpreted as the emission of a baby universe making the black hole younger, and equivalently, reducing the length of the wormhole.

³The time dependence of a 2+1 dimensional Lorentzian wormhole with three AdS boundaries [34] demonstrates non-linear growth that eventually saturates at late times [35].

It is natural to extend the procedure described above to find the transition amplitude from the path integral of a somewhat complex geometry featuring two or more baby universes and non-zero genus. However, a naive generalization of this procedure leads to a puzzling outcome.

To elaborate, let us consider the partition function for a geometry constructed from a trumpet and a three-holed sphere, which can be utilized to study the emission of two baby universes. The corresponding partition function is:

$Z_0(\beta, a_1, a_2,) =$



$$= e^{S_0 \chi} \int_0^\infty Z_{\text{trumpet}}(\beta, a_3) V_{0,3}(a_1, a_2, a_3) a_3 da_3 = e^{S_0 \chi} \frac{\sqrt{\beta}}{\sqrt{\pi}}. \quad (1.5)$$

Here, $V_{0,3}(a_1, a_2, a_3)$ denotes the Weil-Petersson (WP) volume of a geometry with zero genus and three boundaries, where the subscript 0 indicates that the genus of the geometry is zero. Notably, this volume is known to be independent of the lengths a_i : $V_{0,3}(a_1, a_2, a_3) = 1$ [36]⁴. As a result, the path integral becomes independent of the lengths of the baby universes, as demonstrated in the above expression. This raises challenges in interpreting the tunneling process from a black hole to a white hole in the context of this path integral, rendering it somewhat elusive.

This issue may initially seem to stem from the fact that the WP volume of the three-holed sphere is independent of the geodesic lengths. However, it is worth noting that the problem persists even for geometries with arbitrary numbers of geodesic boundaries and genus, because of the structure of the WP volume. In fact, for a geometry with n boundaries and genus g , this volume is a symmetric polynomial function of the squared geodesic lengths $a_1^2, a_2^2, \dots, a_n^2$, with a degree of $3g - 3 + n$. It can be expressed as follows [36, 37]:

$$V_{g,n}(\mathbf{a}) = \sum_{|\alpha| \leq 3g-3+n} c_{g,n}(\alpha) \prod_{j=1}^n \frac{a_j^{2\alpha_j}}{2^{2\alpha_j} (2\alpha_j + 1)!}, \quad (1.6)$$

where $\mathbf{a} = (a_1, \dots, a_n)$ represents the geodesic lengths of the boundaries. Although the complexity of the structure may make it tedious to analyze, it is straightforward to see that the aforementioned problem persists in these cases as well.

This paper aims to present a method for computing the tunneling amplitude from the partition function, building upon the naive procedure discussed earlier. This involves focusing on a specific region of the moduli space. Specifically, we will utilize Kontsevich's approach to compute the WP volume in the Airy limit using ribbon graphs. Our main observation is that, while all associated

⁴The Euler characteristic and the ground state entropy are denoted by χ and S_0 , respectively.

graphs must be considered to compute the WP volume of a geometry with a given genus and boundary in the Airy limit, only certain graphs indicate the tunneling process.

The paper is organized as follows: In the next section, we begin by reviewing Kontsevich's approach to computing the volume of the moduli space. We then explore how the tunneling process can occur within specific regions of the moduli space of a three-holed sphere. Section 3 extends this discussion to other geometries, one involving three baby universes and the other with a single baby universe and a single genus, offering further elaboration on the ideas introduced in Section 2. Finally, concluding remarks are presented in Section 4.

2 Tunneling in a geometry with constant Weil-Petersson volume

In this section, we will study the tunneling amplitude associated with the emission of two baby universes. Building on our discussion in the introduction, we need to revisit the partition function of geometry with one asymptotic boundary and two geodesic boundaries. To achieve this, we will employ Kontsevich's approach to compute the WP volume in the Airy limit, which involves calculating certain ribbon graphs. Utilizing these results, we can determine the contribution of each graph to the partition function. While it is essential to consider the contributions of all graphs to obtain the expected partition function, only some may yield a physically acceptable tunneling amplitude. To proceed, the next subsection briefly reviews Kontsevich's approach to computing the corresponding volume.

2.1 Kontsevich's decomposition of moduli space

To review Kontsevich's approach to computing the WP volume, we consider surfaces of genus g with n geodesic boundaries. In a specific case known as the Airy limit, or thin-strip limit, these boundaries extend indefinitely while the overall area of the surfaces remains fixed. Under this condition, the hyperbolic surfaces transition into what are known as ribbon graphs [38, 39].

In practice, instead of depicting the entire surface, we represent it using a trivalent graph. A trivalent graph is characterized by each vertex connecting exactly three edges. In this representation, lengths are assigned to the edges, while the bulk geometry of the corresponding surface is not explicitly shown. The number of edges E and vertices V in such a graph is given by the following relations:

$$E = 6g - 6 + 3n, \quad V = 4g - 4 + 2n, \quad (2.1)$$

yielding

$$V - E = 2 - 2g - n. \quad (2.2)$$

The above relation is essentially the Euler characteristic formula, which highlights a fundamental property of the graph associated with the ribbon graph structure.

Considering the thin-strip limit offers a useful simplification for analyzing the moduli space,

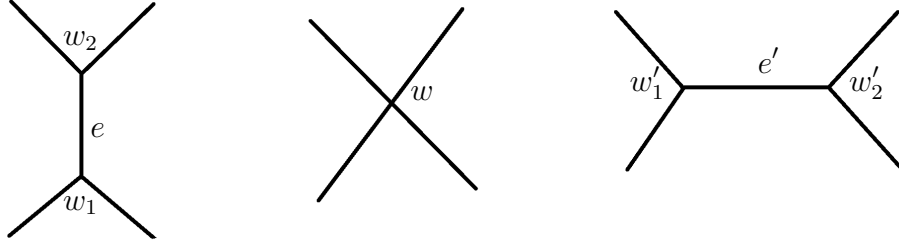


Figure 1: Illustration of the Whitehead collapse process on a graph G , where collapsing an edge e merges vertices w_1 and w_2 into a new vertex w' . In the resulting graph G' , a new edge e' is added in a different direction, forming a trivalent graph.

where the WP volume (1.6) is replaced by the Airy volume, defined as:

$$V_{g,n}^{\text{Airy}}(\mathbf{a}) = \lim_{\Lambda \rightarrow \infty} \Lambda^{3-3g-n} V_{g,n}(\Lambda \mathbf{a}). \quad (2.3)$$

Under this approximation, the moduli space can be expressed as a sum over trivalent ribbon graphs. In this context, we also incorporate an integral that accounts for the lengths of the edges that form these graphs, while ensuring that the lengths of the boundaries are fixed at specified values a_i . Consequently, one arrives at the following expression for the volume in the Airy limit [38, 39]:

$$V_{g,n}^{\text{Airy}}(\mathbf{a}) = \sum_{\Gamma \in \Gamma_{g,n}} \frac{2^{2g-2+n}}{|\text{Aut}(\Gamma_{g,n})|} \prod_{k=1}^E \int_0^\infty dy_k \prod_{i=1}^n \delta\left(a_i - \sum_{k=1}^n n_k^i y_k\right). \quad (2.4)$$

Here, $\Gamma_{g,n}$ denotes the set of trivalent ribbon graphs of genus g and n boundaries, known as Kontsevich graphs. In the above expression y_k is the length of edge k , and $n_i \in \{0, 1, 2\}$ denotes the number of sides of edge k that belong to boundary i .

It is also useful to perform the Laplace transform of the expression (2.4) to obtain:

$$\begin{aligned} \tilde{V}_{g,n}^{\text{Airy}}(\mathbf{z}) &\equiv \int_0^\infty \prod_{i=1}^n da_i e^{-z_i a_i} V_{g,n}^{\text{Airy}}(\mathbf{a}) \\ &= \sum_{\Gamma_{g,n}} \frac{2^{2g-2+n}}{|\text{Aut}(\Gamma_{g,n})|} \prod_{k=1}^E \frac{1}{z_{l(k)} + z_{r(k)}}, \end{aligned} \quad (2.5)$$

that looks simpler and more intuitive for the computation of the WP volume in the Airy limit. Here the $l(k) \in \{1 \dots n\}$ index labels which boundary of the Riemann surface the left side of the ribbon belongs to. Similarly, $r(k)$ labels which boundary the right side of the ribbon belongs to.

To enumerate the graphs, it is useful to note that all orientable graphs for fixed (g, n) can be derived from a single graph through repeated application of the cross operation (or Whitehead collapse). Starting with a trivalent graph G that contains an edge e and two vertices w_1 and

w_2 , one can obtain another trivalent graph G' by merging the vertices w_1 and w_2 into a single vertex w . Subsequently, one can expand in a different direction to create a new edge e' and introduce new vertices w'_1 and w'_2 , as illustrated in figure 1. This entire process is referred to as a Whitehead collapse, which results in a new graph while preserving certain important structural properties [40, 41].

2.2 Geometry with two baby universes

In this subsection, the WP volume of a three-holed sphere with geodesic boundaries denoted by a_1, a_2, a_3 in the Airy limit will be computed using Kontsevich's approach. To begin, all possible ribbon graphs associated with the three-holed sphere must be identified. It is relatively straightforward to show that, in this case, the corresponding graphs consist of three edges and two vertices, leading to the consideration of four specific graphs, as depicted in figure 2. Using the formula (2.4), the contribution of the first Kontsevich graph to the volume $V_{0,3}(a_1, a_2, a_3)$ is:

$$\begin{aligned} V_{0,3}^{\text{I}}(a_1, a_2, a_3) &= 2 \int_0^\infty dy_1 dy_2 dy_3 \delta(y_1 + y_2 + 2y_3 - a_3) \delta(y_1 - a_1) \delta(y_2 - a_2) \\ &= 2 \int_0^\infty dy_3 \delta(a_1 + a_2 + 2y_3 - a_3) = \theta(a_3 - a_1 - a_2). \end{aligned} \quad (2.6)$$

Similarly, the contributions from the second and third Kontsevich graphs can be computed, as they are essentially obtained through permutations of the first graph:

$$V_{0,3}^{\text{II}}(a_1, a_2, a_3) = \theta(a_1 - a_3 - a_2), \quad V_{0,3}^{\text{III}}(a_1, a_2, a_3) = \theta(a_2 - a_1 - a_3). \quad (2.7)$$

The last Kontsevich graph in figure 2, which is symmetric under the permutation of the geodesics, yields the following contribution:

$$\begin{aligned} V_{0,3}^{\text{IV}}(a_1, a_2, a_3) &= 2 \int_0^\infty dy_1 dy_2 dy_3 \delta(y_1 + y_2 - a_3) \delta(y_1 + y_3 - a_1) \delta(y_2 + y_3 - a_2) \\ &= \theta(a_1 + a_2 - a_3) \theta(a_1 - a_2 + a_3) \theta(a_3 - a_1 + a_2), \end{aligned} \quad (2.8)$$

which is also symmetric under the permutation of the geodesics. It follows from the sum of all contributions that

$$V_{0,3}(a_3, a_1, a_2) = \sum_{i=\text{I}}^{\text{IV}} V_{0,3}^i(a_3, a_1, a_2) = 1, \quad (2.9)$$

as expected.

It is also useful to compute the contribution of each Kontsevich graph to the path integral given in (1.5). To do so, one may attach each Kontsevich graph to the trumpet along the geodesic

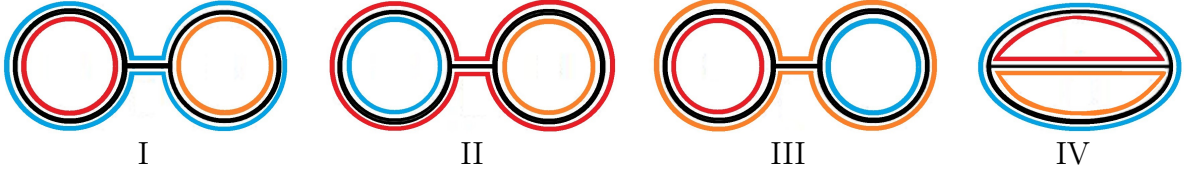


Figure 2: The diagram shows the four trivalent Kontsevich graphs of type $(0, 3)$. The colored curves denote the boundaries of a three-holed sphere: the red curve corresponds to the boundary with length a_1 , the orange curve to the boundary with length a_2 , and the blue curve to the boundary with length a_3 .

a_3 . For the first graph, the contribution is given by:

$$\mathcal{Z}_0^{\text{I}}(\beta, a_1, a_2) = e^{S_0 x} \int_0^\infty Z_{\text{trumpet}}(\beta, a_3) V_{0,3}^{\text{I}}(a_1, a_2, a_3) a_3 da_3 = e^{S_0 x} \frac{\sqrt{\beta}}{\sqrt{\pi}} \exp\left(-\frac{(a_1 + a_2)^2}{4\beta}\right). \quad (2.10)$$

Similarly, the contributions from the other Kontsevich graphs are:

$$\begin{aligned} \mathcal{Z}_0^{\text{II}}(\beta, a_1, a_2) &= e^{S_0 x} \frac{\sqrt{\beta}}{\sqrt{\pi}} \left(1 - \exp\left(-\frac{(a_1 - a_2)^2}{4\beta}\right)\right) \theta(a_1 - a_2), \\ \mathcal{Z}_0^{\text{III}}(\beta, a_1, a_2) &= e^{S_0 x} \frac{\sqrt{\beta}}{\sqrt{\pi}} \left(1 - \exp\left(-\frac{(a_1 - a_2)^2}{4\beta}\right)\right) \theta(a_2 - a_1), \\ \mathcal{Z}_0^{\text{IV}}(\beta, a_1, a_2) &= e^{S_0 x} \frac{\sqrt{\beta}}{\sqrt{\pi}} \left(\exp\left(-\frac{(a_1 - a_2)^2}{4\beta}\right) - \exp\left(-\frac{(a_1 + a_2)^2}{4\beta}\right)\right), \end{aligned} \quad (2.11)$$

It is evident that their sum yields the partition function in (1.5).

As previously mentioned, the partition function of the trumpet can be interpreted as the tunneling amplitude from the thermofield double state of age t to the thermofield double state of age t' , along with a baby universe of size a , after replacing β with $\beta + i(t - t')$. Naturally, this interpretation can be extended to the case where two baby universes are emitted. In this scenario, the tunneling amplitude associated with Kontsevich graph I is given by:

$$\begin{aligned} \langle \text{age } t'; a_1, a_2 | \text{age } t \rangle_{\text{I}} &= e^{S_0 x} \frac{\sqrt{\beta + i(t - t')}}{\sqrt{\pi}} \exp\left(-\frac{(a_1 + a_2)^2}{4(\beta + i(t - t'))}\right) \\ &\approx e^{S_0 x} \frac{\sqrt{i(t - t')}}{\sqrt{\pi}} \exp\left(i \frac{(a_1 + a_2)^2}{4(t - t')} - \beta \frac{(a_1 + a_2)^2}{4(t - t')^2}\right), \end{aligned} \quad (2.12)$$

where the second line corresponds to small β limit with respect to $t - t'$. Moreover, to obtain the amplitude at fixed energy, one may perform an inverse Laplace transformation over β to arrives

at:

$$e^{S_0 x} \frac{\sqrt{i(t-t')}}{\sqrt{\pi}} \exp\left(i \frac{(a_1 + a_2)^2}{4(t-t')}\right) \delta\left(E - \frac{(a_1 + a_2)^2}{4(t-t')^2}\right). \quad (2.13)$$

From the delta function, one obtains:

$$2\sqrt{E}(t-t') = a_1 + a_2, \quad (2.14)$$

indicating that after the emission of baby universes of sizes a_1 and a_2 , the black hole becomes younger, similar to the behavior observed for the trumpet. Applying the same calculation to the Kontsevich graph II (or III) leads to

$$-e^{S_0 x} \frac{\sqrt{i(t-t')}}{\sqrt{\pi}} \exp\left(i \frac{(a_1 - a_2)^2}{4(t-t')}\right) \delta\left(E - \frac{(a_1 - a_2)^2}{4(t-t')^2}\right), \quad (2.15)$$

from which one obtains the following constraint:

$$2\sqrt{E}(t-t') = \pm(a_1 - a_2). \quad (2.16)$$

From this expression, it is evident that it cannot be interpreted as a black hole emitting two baby universes. To illustrate this, one can set $a_1 = a_2$ without loss of generality. Under this assumption, the expression (2.15) becomes zero. Intuitively, one would expect that this assumption—that the two baby universes have the same size—should not lead to a vanishing tunneling amplitude. Therefore, it can be concluded that interpreting the quantity $\mathcal{Z}_0^{\text{II,III}}(\beta, a_1, a_2)$ as a tunneling amplitude is incorrect. From the expression of $\mathcal{Z}_0^{\text{IV}}(\beta, a_1, a_2)$, it is clear that this graph does not introduce any new constraints.

To conclude, the tunneling process of emitting baby universes, which leads to younger black holes, is evident in certain parts of moduli space, particularly in graphs I and IV. However, the sum of their contributions, i.e., the expressions $\mathcal{Z}_0^{\text{I}}(\beta, a_1, a_2)$ and $\mathcal{Z}_0^{\text{IV}}(\beta, a_1, a_2)$, does not show this effect. In contrast, the combined contributions of graphs II, III, and IV do.

The restriction of moduli space has been assumed in the considerations of [21]. The authors introduce a delta function into the path integral of a three-holed sphere, focusing on a specific region of the moduli space associated with firewall geometries. This delta function selects geometries containing wormholes of a particular length to assess the probability of encountering a firewall.

3 Tunneling in geometries with nontrivial Weil-Petersson volumes

To further investigate this approach to computing the tunneling amplitude using the path integral and WP volume, this section examines a black hole emitting three baby universes, corresponding

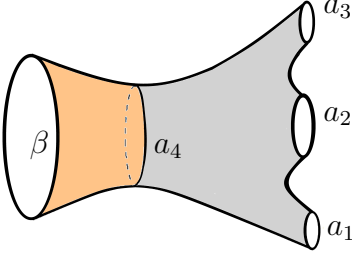
to a four-holed sphere geometry. Additionally, a single-genus geometry with one baby universe is considered, where the genus of the surface introduces a more intricate dependence on the WP volume. In these cases, unlike the three-holed sphere, for which the WP volume remains constant, the WP volumes of these surfaces depend on the parameters that define the geodesic lengths.

3.1 Geometry with three baby universes

The WP volume of a four-holed sphere is given by [36]:

$$V_{0,4}(\mathbf{a}) = 2\pi^2 + \frac{1}{2} \sum_{i=1}^4 a_i^2, \quad (3.1)$$

However, the same puzzle persists: the tunneling amplitude does not explicitly reveal a relationship between the effective age of the black hole and the sizes of the emitted baby universes. To make this more concrete, consider the JT gravity path integral of a geometry with one asymptotic boundary and three geodesic boundaries:

$$\begin{aligned}
 Z_0(\beta, a_1, a_2, a_3) &= \text{Diagram} \\
 &= e^{S_0 \chi} \int_0^\infty Z_{\text{trumpet}}(\beta, a_4) V_{0,4}(a_1, a_2, a_3, a_4) a_4 da_4 \\
 &= e^{S_0 \chi} \frac{\sqrt{\beta}}{2\sqrt{\pi}} (a_1^2 + a_2^2 + a_3^2 + 4(\beta + \pi^2)). \quad (3.2)
 \end{aligned}$$


As can be seen from this expression, the transition amplitude from the black hole to the white hole is not immediately apparent in the above path integral. The goal is to extract a portion of the moduli space that reveals this property.

To proceed, following the analysis in the previous section, we first need to compute the WP volume of the four-holed sphere in the Airy limit using Kontsevich's approach. This involves calculating the contributions from specific six-ribbon graphs, assuming $a_4 > a_1 + a_2 + a_3$ for simplicity, as detailed in Appendix A. Utilizing the results from this appendix, we will examine the path integral (3.2) associated with each ribbon graph. From there, we will derive the transition amplitude and investigate the relationship between the age of the black hole and the lengths of the emitted baby universes.

To begin, we compute the portion of the path integral (3.2) associated with the Kontsevich

graph, which incorporates the WP volume (A.1). This contribution is given by:

$$\begin{aligned} \mathcal{Z}_0^I(\beta, a_1, a_2, a_3) &= e^{S_0 x} \int_0^\infty Z_{\text{trumpet}}(\beta, a_4) V_{0,4}^I(a_1, a_2, a_3, a_4) a_4 da_4 \\ &= e^{S_0 x} c_1 \left\{ \frac{2\beta^{3/2}}{\sqrt{\pi}} \exp\left(-\frac{(a_1 + a_2 + a_3)^2}{4\beta}\right) - \beta (a_1 + a_2 + a_3) \operatorname{erfc}\left(\frac{a_1 + a_2 + a_3}{2\sqrt{\beta}}\right) \right\}. \end{aligned} \quad (3.3)$$

The tunneling amplitude from the thermofield double state of age t to the thermofield double state with age t' , plus baby universes of sizes a_1, a_2 , and a_3 , can be obtained via the analytic continuation $\beta \rightarrow \beta + i(t - t')$ as following:

$$\begin{aligned} \langle \text{age } t'; \mathbf{a} | \text{age } t \rangle_I &= e^{S_0 x} c_1 \left\{ \frac{2(\beta + i(t - t'))^{3/2}}{\sqrt{\pi}} \exp\left(-\frac{(a_1 + a_2 + a_3)^2}{4(\beta + i(t - t'))}\right) \right. \\ &\quad \left. - (a_1 + a_2 + a_3)(\beta + i(t - t')) \operatorname{erfc}\left(\frac{a_1 + a_2 + a_3}{2\sqrt{\beta + i(t - t')}}\right) \right\}. \end{aligned} \quad (3.4)$$

In the low β limit, this expression simplifies to:

$$\begin{aligned} \langle \text{age } t'; \mathbf{a} | \text{age } t \rangle_I &\approx e^{S_0 x} c_1 \left\{ \frac{2(i(t - t'))^{3/2}}{\sqrt{\pi}} \exp\left(i\frac{(a_1 + a_2 + a_3)^2}{4(t - t')} - \beta\frac{(a_1 + a_2 + a_3)^2}{4(t - t')^2}\right) \right. \\ &\quad \left. - (a_1 + a_2 + a_3)i(t - t') \operatorname{erfc}\left(\frac{a_1 + a_2 + a_3}{2\sqrt{i(t - t')}} - \beta\frac{a_1 + a_2 + a_3}{4(i(t - t'))^{3/2}}\right) \right\}. \end{aligned} \quad (3.5)$$

To obtain the amplitude at fixed energy, one may perform an inverse Laplace transformation over β . For the term involving the complementary error function (erfc), the result is:

$$\frac{i}{\pi E} \exp\left(2iE(t - t') \frac{((a_1 + a_2 + a_3)^2 - 2E(t - t')^2)}{(a_1 + a_2 + a_3)^2}\right), \quad (3.6)$$

whereas, the exponential term produces the familiar delta function:

$$\frac{\sqrt{i(t - t')}}{\sqrt{\pi}} \exp\left(i\frac{(a_1 + a_2 + a_3)^2}{4(t - t')}\right) \delta\left(E - \frac{(a_1 + a_2 + a_3)^2}{4(t - t')^2}\right). \quad (3.7)$$

It is also straightforward to compute the contributions from the ribbon graphs outlined in the Appendix, which can establish a relationship between the effective age of the black hole and the length of the baby universe. The contributions from the WP volume of the Kontsevich graphs (A.2), (A.5), and (A.8), under the assumption that $a_4 > a_1 + a_2 + a_3$ for the latter two graphs,

are given respectively by:

$$\begin{aligned}
\mathcal{Z}_0^{\text{II}}(\beta, a_1, a_2, a_3) &= e^{S_0\chi} c_2 \beta \operatorname{erfc} \left(\frac{a_1 + a_2 + a_3}{2\sqrt{\beta}} \right) (a_1 + a_2 + a_3), \\
\mathcal{Z}_0^{\text{IIIA}}(\beta, a_1, a_2, a_3) &= e^{S_0\chi} c_3 \frac{\beta}{4} \left\{ \frac{2\sqrt{\beta}}{\sqrt{\pi}} \left(\exp \left(-\frac{(-a_1 + a_2 + a_3)^2}{4\beta} \right) - \exp \left(-\frac{(a_1 + a_2 + a_3)^2}{4\beta} \right) \right) \right. \\
&\quad \left. + (a_1 - a_2 + a_3) \left(\operatorname{erf} \left(\frac{-a_1 + a_2 + a_3}{2\sqrt{\beta}} \right) - \operatorname{erf} \left(\frac{a_1 + a_2 + a_3}{2\sqrt{\beta}} \right) \right) \right\}, \\
\mathcal{Z}_0^{\text{IIIB}}(\beta, a_1, a_2, a_3) &= e^{S_0\chi} c_3 \beta \left\{ \frac{2\sqrt{\beta}}{\sqrt{\pi}} \left(\exp \left(-\frac{a_1^2}{4\beta} \right) - \exp \left(-\frac{(a_1 - a_2 + a_3)^2}{4\beta} \right) \right) \right. \\
&\quad \left. + a_1 \left(\operatorname{erf} \left(\frac{a_1}{2\sqrt{\beta}} \right) - \operatorname{erf} \left(\frac{a_1 - a_2 + a_3}{2\sqrt{\beta}} \right) \right) \right\}. \tag{3.8}
\end{aligned}$$

As observed with the first graph, the exponential terms yield delta functions, while the terms involving the complementary error function (erfc) do not impose any constraints on the parameters. The corresponding delta functions are:

$$\begin{aligned}
&\frac{\sqrt{i(t-t')}}{\sqrt{\pi}} \exp \left(i \frac{(a_2 - a_1 + a_3)^2}{4(t-t')} \right) \delta \left(E - \frac{(a_2 - a_1 + a_3)^2}{4(t-t')^2} \right), \\
&\frac{\sqrt{i(t-t')}}{\sqrt{\pi}} \exp \left(i \frac{(a_1 - a_2 + a_3)^2}{4(t-t')} \right) \delta \left(E - \frac{(a_1 - a_2 + a_3)^2}{4(t-t')^2} \right). \tag{3.9}
\end{aligned}$$

From the relations (3.7) and (3.9), the following constraints are obtained:

$$\begin{aligned}
2\sqrt{E}(t-t') &= (a_1 + a_2 + a_3), \\
2\sqrt{E}(t-t') &= \pm (a_1 - a_2 + a_3), \\
2\sqrt{E}(t-t') &= \pm (a_2 - a_1 + a_3). \tag{3.10}
\end{aligned}$$

From the above expressions, it can be observed that graphs I and IIIA exhibit the notion of a tunneling process.

If we relax the assumption $a_4 > a_1 + a_2 + a_3$ for the Kontsevich graphs IV and V, they can also be interpreted as representing a tunneling process. This interpretation arises due to the presence of the term:

$$\beta^2 \exp \left(-\frac{(a_1 + a_2 + a_3)^2}{4\beta} \right), \tag{3.11}$$

in their contribution to the path integral (3.2) in the Airy limit.

3.2 Single-genus geometry with a baby universe

It is also insightful to consider the tunneling amplitude for the simplest geometry with a single genus. This includes a Riemann surface of genus one with two boundaries, which, when attached to a trumpet, provides the one-loop correction to the partition function for the emission of a single baby universe, as discussed in the introduction. The motivation for performing this computation is to demonstrate that the issue encountered in the previous section—specifically, that only certain graphs contribute to the amplitude—also arises in this case.

The WP volume of the corresponding geometry is [37]:

$$V_{1,2}(a_1, a_2) = \frac{1}{192} (4\pi^2 + a_1^2 + a_2^2) (12\pi^2 + a_1^2 + a_2^2), \quad (3.12)$$

which results in the partition function:

$$\begin{aligned} Z_1(\beta, a_1) &= \text{Diagram} \\ &= e^{S_0 X} \int_0^\infty Z_{\text{trumpet}}(\beta, a_2) V_{1,2}(a_1, a_2) a_2 da_2 \\ &= e^{S_0 X} \frac{\sqrt{\beta}}{192\sqrt{\pi}} (a_1^4 + 8a_1^2(\beta + 2\pi^2) + 16(2\beta^2 + 4\pi^2\beta + 3\pi^4)). \end{aligned} \quad (3.13)$$

To compute the WP volume $V_{1,2}$ in the Airy limit using Kontsevich's approach, one must consider nine distinct ribbon graphs, as shown in figure (3). This figure is included with permission from [42]. The graphs are labeled by the number of propagators, and their contributions to $\tilde{V}_{1,2}^{\text{Airy}}(z_1, z_2)$ are:

$$\begin{aligned} \tilde{V}_{1,2}^{(0,5)}(a_1, a_2) &= \frac{1}{8z_2^5(z_1 + z_2)}, & V_{1,2}^{(0,4)}(a_1, a_2) &= \frac{1}{8z_2^4(z_1 + z_2)^2} \\ \tilde{V}_{1,2}^{(0,3)}(a_1, a_2) &= \frac{1}{6z_2^3(z_1 + z_2)^3}, & \tilde{V}_{1,2}^{(0,2)}(a_1, a_2) &= \frac{1}{4z_2^2(z_1 + z_2)^4}, \\ V_{1,2}^{(1,1)}(a_1, a_2) &= \frac{1}{2z_1 z_2 (z_1 + z_2)^4} \end{aligned} \quad (3.14)$$

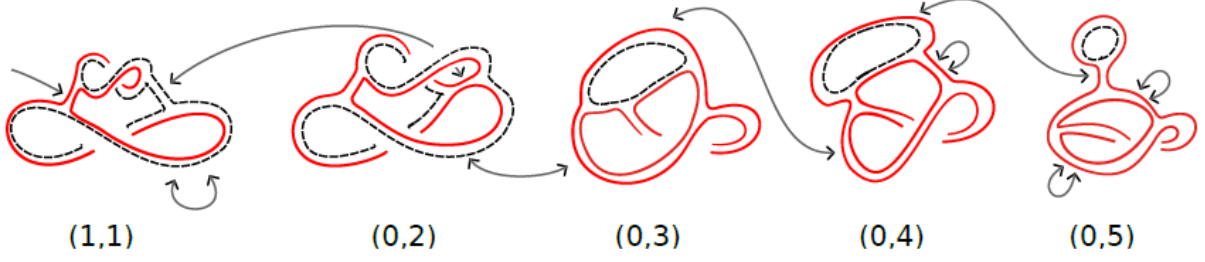


Figure 3: The nine Kontsevich graphs with two boundaries and genus one consist of these five, along with four additional graphs obtained by interchanging the solid (red) and dashed (black) lines in the last four graphs. The dashed (black) lines correspond to boundary 1, while the solid (red) lines correspond to boundary 2. The gray lines with arrows indicate the effect of applying a cross-operation to a given edge.

The WP volume associated with each of these graphs is:

$$\begin{aligned}
V_{1,2}^{(0,5)}(a_1, a_2) &= \frac{1}{192} (a_2 - a_1)^4 \theta(a_2 - a_1), \\
V_{1,2}^{(0,4)}(a_1, a_2) &= \frac{1}{48} (a_2 - a_1)^3 a_1 \theta(a_2 - a_1), \\
V_{1,2}^{(0,3)}(a_1, a_2) &= \frac{1}{24} (a_2 - a_1)^2 a_1^2 \theta(a_2 - a_1), \\
V_{1,2}^{(0,2)}(a_1, a_2) &= \frac{1}{24} (a_2 - a_1) a_1^3 \theta(a_2 - a_1), \\
V_{1,2}^{(1,1)}(a_1, a_2) &= \frac{1}{48} (a_1^4 \theta(a_2 - a_1) + a_2^4 \theta(a_1 - a_2)).
\end{aligned} \tag{3.15}$$

The contributions of other graphs to the volume $V_{1,2}^{\text{Airy}}(a_1, a_2)$ can be determined by swapping a_1 and a_2 . The contribution of each graph to the path integral (3.13) can be derived from the volumes mentioned above, which are:

$$\begin{aligned}
\mathcal{Z}_1^{(0,5)}(\beta, a_1) &= \frac{1}{48} \beta \left(\frac{2\sqrt{\beta}(a_1^2 + 4\beta)}{\sqrt{\pi}} \exp\left(-\frac{a_1^2}{4\beta}\right) - a_1 (a_1^2 + 6\beta) \operatorname{erfc}\left(\frac{a_1}{2\sqrt{\beta}}\right) \right), \\
\mathcal{Z}_1^{(0,4)}(\beta, a_1) &= \frac{1}{16} \beta a_1 \left((a_1^2 + 2\beta) \operatorname{erfc}\left(\frac{a_1}{2\sqrt{\beta}}\right) - \frac{2\sqrt{\beta}a_1}{\sqrt{\pi}} \exp\left(-\frac{a_1^2}{4\beta}\right) \right), \\
\mathcal{Z}_1^{(0,3)}(\beta, a_1) &= \frac{\beta^{3/2} a_1^2}{6\sqrt{\pi}} \exp\left(-\frac{a_1^2}{4\beta}\right) - \frac{1}{12} \beta a_1^3 \operatorname{erfc}\left(\frac{a_1}{2\sqrt{\beta}}\right), \\
\mathcal{Z}_1^{(0,2)}(\beta, a_1) &= \frac{1}{24} \beta a_1^3 \operatorname{erfc}\left(\frac{a_1}{2\sqrt{\beta}}\right), \\
\mathcal{Z}_1^{(1,1)}(\beta, a_1) &= \frac{\beta^{3/2}}{6\sqrt{\pi}} \left(4\beta - \exp\left(-\frac{a_1^2}{4\beta}\right) (a_1^2 + 4\beta) \right).
\end{aligned} \tag{3.16}$$

The above expressions reveal that Kontsevich graphs which contain the term $\exp\left(-\frac{a_1^2}{4\beta}\right)$ relate

the black hole's age to the baby universe's length. Explicitly, the path integral $\mathcal{Z}_1^{(0,2)}(\beta, a_1)$ does not exhibit the feature of baby universe emission. One can also see that other graphs whose volume can be obtained by swapping a_1 and a_2 in (3.15), exhibit this feature.

4 Concluding remarks

In this paper, Jackiw-Teitelboim gravity path integrals were explored, focusing particularly on the tunneling process between aging and younger black holes through the emission of baby universes. The main motivation for studying this subject was to better understand the relationship between the effective age of a black hole and the geometrical structures formed due to these tunneling processes. By examining the path integrals for geometries with more complex structures, including those with higher-genus structures and multiple geodesic boundaries, an attempt was made to provide a clear explanation of the physical implications of these quantum gravity effects.

The main observation is that while the path integral of the trumpet geometry in Jackiw-Teitelboim gravity can be interpreted as a tunneling amplitude, this interpretation becomes less straightforward for geometries with multiple baby universes and nontrivial Weil-Petersson volumes. Indeed, by making use of Kontsevich's approach, which utilizes ribbon graphs to compute Weil-Petersson volumes in the Airy limit, specific regions of the moduli space that meaningfully contribute to the tunneling process were identified. This approach allowed for the extraction of transition amplitudes that directly relate the emission of baby universes to the effective age of black holes.

In fact, it has been demonstrated that not all contributions to the Weil-Petersson volume correspond to a physically meaningful tunneling process. Only certain Kontsevich graphs exhibited the expected relationship between black hole age and baby universe emission. This finding highlights the need to restrict moduli space considerations to specific configurations that contribute to observable physical phenomena. This restriction is in agreement with the study by Stanford and Yang [21], which introduced a delta function into the path integral of the three-holed sphere to focus on specific regions of the moduli space associated with firewall geometries (see also [26] for the case of a five-holed sphere). This delta function isolates geometries containing wormholes of specific lengths to calculate the probability of encountering a firewall.

These results help to better understand how black holes change over time. The creation of baby universes makes black holes younger and offers a simpler way to approach the black hole information problem and the nature of space-time connectivity. Moreover, these results may suggest that this procedure is highly sensitive to the underlying geometric constraints, implying that not all configurations contribute equally to observable quantum processes.

Acknowledgments

We thank Seyed Amirhossein Mousavi, Reza Pirmoradian, Mohammad Reza Tanhaei, and Mohammad Javad Vasli for their valuable support and insightful discussions. The work of M.

A. is supported by the Iran National Science Foundation (INSF) under project No. 4023620. Additionally, OpenAI's ChatGPT was used to enhance the clarity of this manuscript.

A Kontsevich graphs of four-holed sphere

To derive the WP volume given in equation (3.1) at the Airy limit, one should consider Kontsevich graphs with six edges and four vertices. The geodesic boundaries a_1, a_2, a_3 and a_4 are indicated in the ribbon graphs by curves colored green, orange, blue, and red, respectively. In the simplest form of a ribbon graph, geodesic boundaries a_1, a_2 and a_3 , are symmetric in their roles, while the geodesic boundary a_4 is bigger than the sum $a_1 + a_2 + a_3$. The Laplace transform of the WP volume of this graph is:

$$\tilde{V}_{0,4}^I(\mathbf{z}) = \frac{1}{z_3 + z_4} \frac{1}{z_2 + z_4} \frac{1}{2z_4} \frac{1}{2z_4} \frac{1}{z_1 + z_4}$$

Figure 4: In Kontsevich graph I, the geodesic boundaries a_1, a_2 , and a_3 display similar behavior, while a_4 behaves differently.

Following the application of the inverse Laplace transform, the result is:

$$\begin{aligned} V_{0,4}^I(\mathbf{a}) &= \int_{\gamma+i\mathbb{R}} \prod_{i=1}^4 \frac{dz_i}{2\pi i} e^{a_i z_i} \frac{c_1}{z_4^3 (z_1 + z_4) (z_2 + z_4) (z_3 + z_4)} \\ &= \frac{c_1}{2} (a_1 + a_2 + a_3 - a_4)^2 \theta(a_4 - a_1 - a_2 - a_3). \end{aligned} \quad (\text{A.1})$$

The coefficients c_i (for $i = 1, \dots, 5$) are determined by the symmetry factor of each ribbon graph. As expected from figure 4 and the previous result, it is clear that a_1, a_2 and a_3 display similar behavior, while a_4 behaves differently in $V_{0,4}^I$. Due to the presence of the theta function in $V_{0,4}^I$, we will focus on configurations of ribbon graphs that produce this theta function to simplify the derivation of (3.1) in the Airy limit.

To construct a new Kontsevich graph, starting from graph I, one can first collapse the vertical edge, merging the two vertices into a single vertex. Subsequently, one obtains ribbon graph II by expanding this new vertex along the horizontal direction (see figure 5). In this ribbon graph,

the contribution of the geodesic boundary a_2 in $V_{0,4}^{\text{II}}(\mathbf{z})$ differs from that of a_1 and a_3 and the power of propagator $1/z_4$ decreases by one order.

$$V_{0,4}^{\text{II}}(\mathbf{z}) = \frac{1}{z_3 + z_4} \left(\text{Diagram} \right) \frac{1}{z_1 + z_4}$$

Figure 5: In Kontsevich graph II, the geodesic boundaries a_1 and a_2 display similar behavior, while a_3 and a_4 behaves differently.

The contribution of ribbon graph II to the volume is:

$$\begin{aligned} V_{0,4}^{\text{II}}(\mathbf{a}) &= \int_{\gamma+i\mathbb{R}} \prod_{i=1}^4 \frac{dz_i}{2\pi i} e^{a_i z_i} \frac{c_2}{z_4^2 (z_1 + z_4) (z_2 + z_4)^2 (z_3 + z_4)} \\ &= c_2 a_2 (a_4 - a_1 - a_2 - a_3) \theta(a_4 - a_1 - a_2 - a_3). \end{aligned} \quad (\text{A.2})$$

If a_2 is replaced with a_1 and a_3 , the total contribution of this configuration to the volume is:

$$V_{0,4}^{\text{II}_{\text{total}}}(\mathbf{a}) = c_2 (a_1 + a_2 + a_3) (a_4 - a_1 - a_2 - a_3) \theta(a_4 - a_1 - a_2 - a_3). \quad (\text{A.3})$$

The Whitehead method is now applied again to obtain another ribbon graph. By contracting the left horizontal edge of ribbon graph II and expanding vertically, ribbon graph IIIA is obtained (see figure 6).

$$\tilde{V}_{0,4}^{\text{IIIA}}(\mathbf{z}) = \frac{1}{z_1 + z_4} \left(\text{Diagram} \right) \frac{1}{z_3 + z_4}$$

Figure 6: Kontsevich graph IIIA

In this graph, the power of $1/z_4$ is one and its contribution to the volume of moduli space is:

$$\begin{aligned}
V_{0,4}^{\text{IIIA}}(\mathbf{a}) &= \int_{\gamma+i\mathbb{R}} \prod_{i=1}^4 \frac{dz_i}{2\pi i} e^{a_i z_i} \frac{c_3}{z_4 (z_1 + z_4) (z_1 + z_2) (z_2 + z_4)^2 (z_3 + z_4)} \\
&= \frac{c_3}{8} \left\{ (a_1 - a_2 + a_3 - a_4)^2 \theta(a_1 - a_2, a_4 - a_1 + a_2 - a_3) \right. \\
&\quad + 4a_2 (a_1 + a_2 + a_3 - a_4) \theta(a_4 - a_1 - a_2 - a_3) \\
&\quad - (a_1 + a_2 + a_3 - a_4)^2 \theta(a_4 - a_1 - a_2 - a_3) \\
&\quad - (a_1 - a_2 - a_3 + a_4)^2 \theta(a_1 - a_2, a_1 - a_2 - a_3 + a_4) \\
&\quad + 4a_2 (-a_1 + a_2 + a_3 - a_4) \theta(a_1 - a_2, a_1 - a_2 - a_3 + a_4) \\
&\quad + 4a_1 (a_1 - a_2 - a_3 + a_4) \theta(a_1 - a_2, a_1 - a_2 - a_3 + a_4) \\
&\quad + (a_1 - a_2 - a_3 + a_4)^2 \theta(a_1 - a_2 - a_3 + a_4) \\
&\quad + 4a_1 (-a_1 + a_2 + a_3 - a_4) \theta(a_1 - a_2 - a_3 + a_4) \\
&\quad \left. + 4a_2 (a_1 - a_2 - a_3 + a_4) \theta(a_1 - a_2 - a_3 + a_4) \right\}. \tag{A.4}
\end{aligned}$$

Assuming $a_4 > a_3 + a_2 + a_1$, the relation above simplifies to:

$$V_{0,4}^{\text{IIIA}}(\mathbf{a}) = \frac{c_3}{2} \left\{ a_2^2 \theta(a_1 - a_2) - a_1 (a_1 - 2a_2) \theta(a_2 - a_1) \right\}, \tag{A.5}$$

and other permutations among the geodesic boundaries yield:

$$c_3 \left\{ a_1 a_2 + a_1 a_3 + a_2 a_3 \right\}. \tag{A.6}$$

Another configuration, similar to graph IIIA, also includes the propagator $1/z_4$ (see figure 7). However, this configuration differs from graph IIIA due to variations in the orientations of the geodesic boundaries. For clarification, consider expression (A.1) for graph I, where $1/z_4^3$ ensures that $a_4 > a_3$, $a_4 > a_2$, and $a_4 > a_1$. In graph II, $1/z_4^2$ appears, while in graph IIIA, expression (A.4) contains $1/z_4$. The presence of $1/z_4^n$ ($n = 1, 2, 3$) in these expressions is crucial. For simplicity, the analysis of the ribbon graphs is restricted to the condition $\theta(a_4 - a_1 - a_2 - a_3)$, where ribbon graphs containing propagators $1/z_4^n$ contribute to this condition. In ribbon graphs IV and V (see figures 8 and 9), no $1/z_4^n$ terms are present, and their contributions are zero. Interestingly, graph IIIB contributes similarly to IIIA, as both contain $1/z_4$, in contrast to graph II, which contains $1/z_4^2$.

$$\tilde{V}_{0,4}^{\text{III B}}(\mathbf{z}) = \frac{1}{z_3 + z_4} \left(\text{Diagram} \right) \frac{1}{z_2 + z_3}$$

Figure 7: Kontsevich graph III B

The WP volume of this graph is:

$$\begin{aligned} V_{0,4}^{\text{III B}}(\mathbf{a}) &= \int_{\gamma+i\mathbb{R}} \prod_{i=1}^4 \frac{dz_i}{2\pi i} e^{a_i z_i} \frac{1}{z_3 (z_2 + z_3) z_4 (z_1 + z_4) (z_3 + z_4)^2} \\ &= \frac{\tilde{c}_3}{2} \theta(a_3 - a_2) \left((a_1 - a_4)^2 \theta(a_4 - a_1) - (a_1 + a_2 - a_3 - a_4) \right. \\ &\quad \left. \times (a_1 - a_2 + a_3 - a_4) \theta(a_4 - a_1 + a_2 - a_3) \right). \end{aligned} \quad (\text{A.7})$$

For the case $a_4 > a_3 + a_2 + a_1$ and $a_3 > a_2 > a_1$ the above expression simplifies to:

$$V_{0,4}^{\text{III B}}(\mathbf{a}) = \frac{\tilde{c}_3}{2} (a_2^2 - 2a_2 a_3 + a_3^2). \quad (\text{A.8})$$

Considering all permutations gives:

$$\tilde{c}_3 \left\{ a_1^2 + a_2^2 + a_3^2 - a_1 a_2 - a_1 a_3 - a_2 a_3 \right\}. \quad (\text{A.9})$$

By setting $c_3 = 2\tilde{c}_3$, and using equations (A.6) and (A.9), we obtain:

$$V_{0,4}^{\text{III total}}(\mathbf{a}) = \frac{c_3}{2} \left\{ a_1^2 + a_2^2 + a_3^2 + a_1 a_2 + a_1 a_3 + a_2 a_3 \right\}. \quad (\text{A.10})$$

We can also consider two additional Kontsevich graphs that do not include the $1/z_4$ factor. Hence, the contribution of these graphs to the volume of the moduli space is zero by the assumption $a_4 > a_3 + a_2 + a_1$ (see figures 8 and 9).

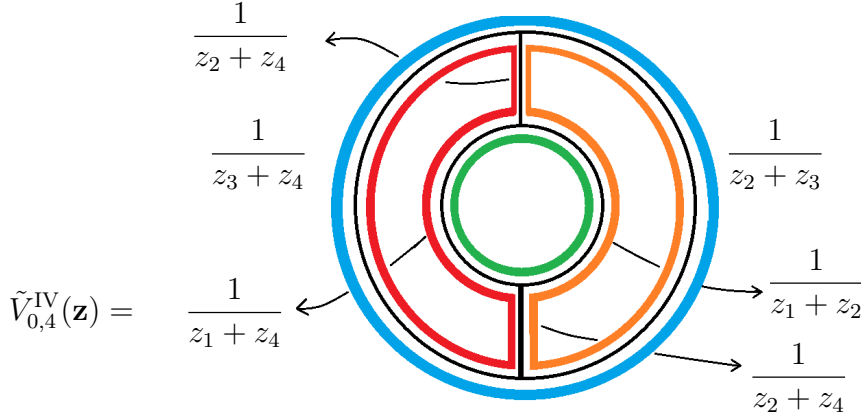


Figure 8: Kontsevich graph IV

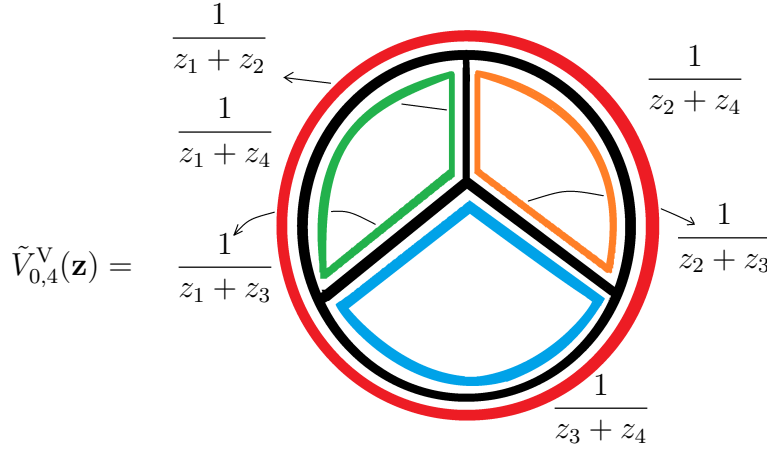


Figure 9: Kontsevich graph V

By summing the contributions of all volumes in (A.1), (A.3), and (A.10), and with c_1 set equal to c_2 and c_3 set to 2, the following result is obtained:

$$V_{0,4}^{\text{Airy}} = \frac{1}{2} (a_1^2 + a_2^2 + a_3^2 + a_4^2) \theta(a_4 - a_1 - a_2 - a_3). \quad (\text{A.11})$$

References

- [1] S. Hawking, “Quantum coherence down the wormhole,” *Physics Letters B* **195** no. 3, (1987) 337–343. <https://www.sciencedirect.com/science/article/pii/0370269387900281>.
- [2] G. V. Lavrelashvili, V. A. Rubakov, and P. G. Tinyakov, “Disruption of Quantum Coherence upon a Change in Spatial Topology in Quantum Gravity,” *JETP Lett.* **46** (1987) 167–169.
- [3] J. M. Maldacena and L. Maoz, “Wormholes in AdS,” *JHEP* **02** (2004) 053, [arXiv:hep-th/0401024](https://arxiv.org/abs/hep-th/0401024).

- [4] N. Arkani-Hamed, J. Orgera, and J. Polchinski, “Euclidean wormholes in string theory,” *JHEP* **12** (2007) 018, [arXiv:0705.2768 \[hep-th\]](#).
- [5] P. Saad, S. H. Shenker, and D. Stanford, “A semiclassical ramp in SYK and in gravity,” [arXiv:1806.06840 \[hep-th\]](#).
- [6] S. D. Mathur, “The Information paradox: A Pedagogical introduction,” *Class. Quant. Grav.* **26** (2009) 224001, [arXiv:0909.1038 \[hep-th\]](#).
- [7] A. Almheiri, D. Marolf, J. Polchinski, and J. Sully, “Black Holes: Complementarity or Firewalls?,” *JHEP* **02** (2013) 062, [arXiv:1207.3123 \[hep-th\]](#).
- [8] R. Bousso, “Complementarity Is Not Enough,” *Phys. Rev. D* **87** no. 12, (2013) 124023, [arXiv:1207.5192 \[hep-th\]](#).
- [9] Y. Nomura, J. Varela, and S. J. Weinberg, “Complementarity Endures: No Firewall for an Infalling Observer,” *JHEP* **03** (2013) 059, [arXiv:1207.6626 \[hep-th\]](#).
- [10] E. Verlinde and H. Verlinde, “Black Hole Entanglement and Quantum Error Correction,” *JHEP* **10** (2013) 107, [arXiv:1211.6913 \[hep-th\]](#).
- [11] K. Papadodimas and S. Raju, “An Infalling Observer in AdS/CFT,” *JHEP* **10** (2013) 212, [arXiv:1211.6767 \[hep-th\]](#).
- [12] R. Jackiw, “Lower dimensional gravity,” *Nuclear Physics B* **252** (1985) 343–356. <https://www.sciencedirect.com/science/article/pii/0550321385904481>.
- [13] C. Teitelboim, “Gravitation and Hamiltonian Structure in Two Space-Time Dimensions,” *Phys. Lett. B* **126** (1983) 41–45.
- [14] Z. Yang, “The Quantum Gravity Dynamics of Near Extremal Black Holes,” *JHEP* **05** (2019) 205, [arXiv:1809.08647 \[hep-th\]](#).
- [15] A. Kitaev and S. J. Suh, “Statistical mechanics of a two-dimensional black hole,” *JHEP* **05** (2019) 198, [arXiv:1808.07032 \[hep-th\]](#).
- [16] D. Bagrets, A. Altland, and A. Kamenev, “Power-law out of time order correlation functions in the SYK model,” *Nucl. Phys. B* **921** (2017) 727–752, [arXiv:1702.08902 \[cond-mat.str-el\]](#).
- [17] D. Harlow and D. Jafferis, “The Factorization Problem in Jackiw-Teitelboim Gravity,” *JHEP* **02** (2020) 177, [arXiv:1804.01081 \[hep-th\]](#).
- [18] P. Saad, S. H. Shenker, and D. Stanford, “JT gravity as a matrix integral,” [arXiv:1903.11115 \[hep-th\]](#).

- [19] D. Stanford and E. Witten, “JT gravity and the ensembles of random matrix theory,” *Adv. Theor. Math. Phys.* **24** no. 6, (2020) 1475–1680, [arXiv:1907.03363 \[hep-th\]](#).
- [20] E. Witten, “Matrix Models and Deformations of JT Gravity,” *Proc. Roy. Soc. Lond. A* **476** no. 2244, (2020) 20200582, [arXiv:2006.13414 \[hep-th\]](#).
- [21] D. Stanford and Z. Yang, “Firewalls from wormholes,” [arXiv:2208.01625 \[hep-th\]](#).
- [22] P. Saad, “Late Time Correlation Functions, Baby Universes, and ETH in JT Gravity,” [arXiv:1910.10311 \[hep-th\]](#).
- [23] S. B. Giddings and A. Strominger, “Axion Induced Topology Change in Quantum Gravity and String Theory,” *Nucl. Phys. B* **306** (1988) 890–907.
- [24] S. Coleman, “Black holes as red herrings: Topological fluctuations and the loss of quantum coherence,” *Nuclear Physics B* **307** no. 4, (1988) 867–882.
<https://www.sciencedirect.com/science/article/pii/0550321388901101>.
- [25] L. Susskind, “The Typical-State Paradox: Diagnosing Horizons with Complexity,” *Fortsch. Phys.* **64** (2016) 84–91, [arXiv:1507.02287 \[hep-th\]](#).
- [26] H. Zolfi, “Firewalls from wormholes in higher genus,” *JHEP* **05** (2024) 039, [arXiv:2401.04476 \[hep-th\]](#).
- [27] T. Hartman and J. Maldacena, “Time Evolution of Entanglement Entropy from Black Hole Interiors,” *JHEP* **05** (2013) 014, [arXiv:1303.1080 \[hep-th\]](#).
- [28] L. Susskind, “Computational Complexity and Black Hole Horizons,” *Fortsch. Phys.* **64** (2016) 24–43, [arXiv:1403.5695 \[hep-th\]](#). [Addendum: *Fortsch.Phys.* 64, 44–48 (2016)].
- [29] L. V. Iliesiu, M. Mezei, and G. Sárosi, “The volume of the black hole interior at late times,” *JHEP* **07** (2022) 073, [arXiv:2107.06286 \[hep-th\]](#).
- [30] M. Alishahiha and S. Banerjee, “On the saturation of late-time growth of complexity in supersymmetric JT gravity,” *JHEP* **01** (2023) 134, [arXiv:2209.02441 \[hep-th\]](#).
- [31] L. V. Iliesiu, A. Levine, H. W. Lin, H. Maxfield, and M. Mezei, “On the non-perturbative bulk Hilbert space of JT gravity,” [arXiv:2403.08696 \[hep-th\]](#).
- [32] A. Belin, R. C. Myers, S.-M. Ruan, G. Sárosi, and A. J. Speranza, “Does Complexity Equal Anything?,” *Phys. Rev. Lett.* **128** no. 8, (2022) 081602, [arXiv:2111.02429 \[hep-th\]](#).
- [33] A. Blommaert, C.-H. Chen, and Y. Nomura, “Firewalls at exponentially late times,” *JHEP* **10** (2024) 131, [arXiv:2403.07049 \[hep-th\]](#).
- [34] K. Skenderis and B. C. van Rees, “Holography and wormholes in 2+1 dimensions,” *Commun. Math. Phys.* **301** (2011) 583–626, [arXiv:0912.2090 \[hep-th\]](#).

- [35] H. Zolfi, “Complexity and Multi-boundary Wormholes in $2 + 1$ dimensions,” *JHEP* **04** (2023) 076, [arXiv:2302.07522 \[hep-th\]](#).
- [36] M. Mirzakhani, “Weil-Petersson volumes and intersection theory on the moduli space of curves,” *J. Am. Math. Soc.* **20** no. 01, (2007) 1–24.
- [37] M. Mirzakhani, “Simple geodesics and Weil-Petersson volumes of moduli spaces of bordered Riemann surfaces,” *Invent. Math.* **167** no. 1, (2006) 179–222.
- [38] M. Kontsevich, “Intersection theory on the moduli space of curves and the matrix airy function,” *Communications in Mathematical Physics* **147** (1992) 1–23.
- [39] N. N. V. Do, “Intersection theory on moduli space of curves via hyperbolic geometry,” *PhD Thesis, The University of Melbourne*, (2008) .
- [40] J. H. Whitehead, “On equivalent sets of elements in a free group,” *Annals of mathematics* **37** no. 4, (1936) 782–800.
- [41] R. C. Penner, “Perturbative series and the moduli space of riemann surfaces,” *Journal of Differential Geometry* **27** no. 1, (1988) 35–53.
- [42] P. Saad, D. Stanford, Z. Yang, and S. Yao, “A convergent genus expansion for the plateau,” [arXiv:2210.11565 \[hep-th\]](#).